Thermodynamic study of the complexation of humic acid by calorimetry

doi: 10.1016/j.jct.2019.01.011

Manuscript for the *Journal of Chemical Thermodynamics*

Thermodynamic study of the complexation of humic acid by calorimetry

Shingo Kimuro[1, 2], Akira Kirishima[1*], Yoshihiro Kitatsuji[3], Kazuya Miyakawa[4], Daisuke Akiyama[1], and Nobuaki Sato[1]

1. Institute of Multidisciplinary Research for Advanced Materials, Tohoku University, 1-1 Katahira, 2-Chome, Aoba-ku, Sendai 980-8577, Japan.
2. Present address: Sector of Nuclear Fuel, Decommissioning, and Waste Management Technology Development, Japan Atomic Energy Agency, 4-32 Muramatsu, Tokai-mura, Naka-gun, Ibaraki 319-1194, Japan.
3. Research group for Analytical Chemistry, Nuclear Chemistry Division, Nuclear Science and Engineering Center, Japan Atomic Energy Agency, 2-4 Shirakata, Tokai-mura, Naka-gun, Ibaraki 319-1195, Japan.
4. Horonobe Underground Research Center, Japan Atomic Energy Agency, 432-2 Hokushin, Horonobe-cho, Teshio-gun, Hokkaido 098-3224, Japan.

* Corresponding author.

Contents

Text pages	51 (excluding this page)
Tables	4 (+ Supplemental material 12)
Figures	9 (Supplemental material 1)

Corresponding author	Akira Kirishima
Address	Institute of Multidisciplinary Research for Advanced Materials, Tohoku University, 1,1, Katahira 2, Sendai 980-8577, Japan
Tel.:	+81-22-217-5143
Fax.:	+81-22-217-5143
E-mail:	kiri@tohoku.ac.jp

Abstract

Although the thermodynamic quantities (Gibbs free energy, reaction enthalpy, and entropy) of the complexation of humic acid are necessary for the discussion of the reaction thermodynamics, their accurate determination, especially concerning dissolved humic acid in deep groundwater, has not been carried out. In this study, a combination of potentiometry and calorimetry was used for the determination of the thermodynamic values of complexation of typical humic acid and groundwater humic acid, which was isolated from deep groundwater at Horonobe, Hokkaido, Japan, with copper (II) ions and uranyl (VI) ions. The apparent complexation constant of Horonobe humic acid was independent of the pH of the bulk solution, whereas that of typical humic acid was dependent on the pH. This observation indicates that the polyelectrolyte effect of Horonobe humic acid is negligible because of its relatively small molecular size. In addition, the effect of the heterogeneity of Horonobe humic acid was not significant. Moreover, the complexation enthalpy of Horonobe humic acid was consistent with that of homogeneous poly(acrylic acid), which means the complexation of Horonobe humic acid was not affected by the functional group heterogeneity. Consequently, the unique complexation mechanism of Horonobe humic acid was revealed based on the determined thermodynamic quantities. The migration of radionuclides in the deep underground environment must be affected by these characteristics; thus, the accurate determination of thermodynamic quantities

of in situ humic substances is very helpful for the safety assessment of geological disposal, when disposal sites for radioactive waste are chosen.

KEYWORDS: humic acid, isothermal titration calorimetry, complexation enthalpy, reaction mechanism

1. Introduction

As components of dissolved organic materials in the groundwater, humic and fulvic acids are of significant importance in the environmental behavior of metals [1–3]. Humic acid is known to be a heterogeneous mixture of high-molecular-weight compounds with many functional groups. In particular, the carboxylic acid groups and phenolic hydroxyl groups interact strongly with metal cations by complex formation. Furthermore, the presence of humic and fulvic acid has been confirmed deep underground in locations where the disposal of radioactive waste is planned. For this reason, numerous attempts have been carried out to model and describe the interactions of humic acid (HA) with metal cations quantitatively [4–10]. Most studies have attempted thermodynamic interpretation by estimating the corresponding equilibrium reactions and have tried to develop models to explain the impact of the polyelectrolyte effect and the heterogeneity of humic acid on the complexation reaction. However, the reaction enthalpy and reaction entropy for humic acid complexation are only estimated values obtained from the equilibrium constants at different temperatures. In contrast, the accurate determination of these thermodynamic quantities is necessary for the discussion of reaction thermodynamics.

Isothermal titration calorimetry is a powerful tool for the direct determination of the reaction enthalpy from the reaction heat. In our previous study, calorimetry was applied to the analysis of the protonation of several humic acids [11], as well as deep-groundwater humic acid obtained

75 at 350 m depth in Horonobe, Hokkaido, Japan [12]. This study allowed us to cultivate a better
76 understanding of the reaction mechanism of humic acid using thermodynamic quantities. These
77 studies revealed that the protonation mechanism of deep groundwater humic acid of Horonobe
78 is similar to that of a mixture of simple organic acids, such as benzoic acid and phenol, whereas
79 the protonation of typical humic acids is characterized by the polyelectrolyte effect and
80 heterogeneity. This unique property of Horonobe humic acid is caused by the relatively small
81 molecular weight, size, and simple structure, which is a result of the long-term thermal and
82 biochemical degradation of organic materials.

83 In terms of the application of calorimetry to the complexation of humic acid, Rao et al [13]
84 reported the complexation enthalpy of humic acid with neptunium (V), Antonelli et al. [14] and
85 Alexandre et al. [15] reported the complexation enthalpy with copper (II), and Du et al. reported
86 the adsorption of copper (II) with humic acid [16]. Most of these studies estimated the
87 equilibrium constant as a constant or discontinuous value by using near-IR adsorption
88 spectrophotometry or batch experiments, although the equilibrium constants of humic acids are
89 continuously affected by the pH, ionic strength, and metal ion concentration. Additionally, there
90 have been no studies about the complexation thermodynamics of very deep (over 300 m from
91 surface) groundwater humic substances in Japan, whereas the geological disposal of radioactive
92 waste is expected to be conducted at such depths. Therefore, the apparent complexation

93 constants of typical and deep groundwater humic acid with Cu (II) ions were determined in this
94 study using a model equation [17], which describes the effects of polyelectrolytes and functional
95 group heterogeneity on the equilibrium constants, based on potentiometric titration using an
96 ion-selective electrode (ISE) for Cu (II) ions; subsequently, the complexation enthalpy and
97 entropy were determined by calorimetry. It is known that Cu (II) ion tends to form covalent
98 bonds with functional groups. In contrast, Uranyl (VI) ions, which is described below, tends to
99 form ionic bonds with them. For this reason, the comparison of complexation enthalpies of Cu
100 (II) and Uranyl (VI) is very helpful for the understanding of reaction mechanism.

101 Uranyl (VI) ions are one of the most important ions in the safety assessment of the geological
102 disposal of spent nuclear fuel, and also important for that of high level radioactive waste (HLW),
103 mainly because of their high solubility and ease of complexation in aqueous systems. Previous
104 efforts revealed that typical humic substances have a high complexation capability with uranyl
105 (VI) ions [18–22]. Thus, the application of models of humic substances to the interaction with
106 uranyl (VI) ions was investigated [19, 23–26]. One experimental difficulty is the undefined
107 complexation constant of humic substances; this value is affected by the pH, ionic strength, and
108 metal ion concentration of the bulk solution because of the polyelectrolyte effect and
109 heterogeneity of the humic acid molecules. Kitatsuji et al. proposed a liquid-membrane-type ISE
110 for plutonium (III) ions [27], which has the advantage of the direct detection of metal ion

111 concentration based on the electric potential. In this study, this plutonium (III) ISE applied to the
112 complexation study of humic substances with uranyl (VI) ions, and the apparent complexation
113 constants of typical and deep groundwater humic acids were determined. Subsequently, the
114 complexation enthalpy and entropy were determined by the calorimetry.
115 Hence, the complexation mechanism of the typical and the deep groundwater humic acids are
116 discussed based on the thermodynamic quantities, which were determined by the direct
117 measurement of the reaction heat. Consequently, the effects of ion complexation on deep
118 groundwater humic acid, such as that obtained from Horonobe, was revealed.
119

120 **2. Experimental**

121 2.1 Materials and sample preparation

122 The Horonobe underground research laboratory (URL) is located in northwestern Hokkaido
123 on the eastern margin of a Neogene-to-Quaternary sedimentary basin. Groundwater was
124 sampled from the horizontal borehole labeled 12-P350-M01 drilled from the 350 m gallery,
125 whose geology is that of the Wakkanai formation (Neogene siliceous mudstones containing opal-
126 CT). Dissolved humic acid in the groundwater was isolated by a protocol using DAX-8 resin, as
127 recommended by the International Humic Substances Society (IHSS). Details of the procedure
128 and the characterization of the Horonobe deep groundwater humic acid is shown in Table S. 1 in

129 supplementary material, which have been described previously [12]. Hereafter, the humic acid
130 isolated from groundwater at 350-m depth is denoted HHA. For a comparison of the differences
131 based on the origin of the humic acid, a standard humic acid “Elliot Soil (Cat. No. 1S102H)”
132 sample, extracted from fertile prairie soil, was purchased from IHSS. This humic acid is denoted
133 SHA in this paper. It was revealed that the molecular size of HHA is obviously smaller than SHA
134 [12]. **Fig. S. 1** in supplementary material indicates the molecular weight distribution of HHA and
135 SHA determined by the total organic carbon (TOC) measurement. The small molecular size of
136 HHA means the small contribution of polyelectrolyte effect in the interaction with cations.
137 Additionally, poly(acrylic acid) (PAA), which mimics the polyelectrolyte effect of humic acid but
138 has a homogeneous molecular structure, was used. The molecular weight of PAA is 90,000. Each
139 humic acid sample and PAA were dissolved in standardized 0.1 mol/dm^3 sodium hydroxide
140 solution and, then, neutralized with an adequate amount of standardized perchloric or
141 hydrochloric acids.

142 Bis(diphenylphosphoryl)methane (BDPPM) was prepared for use as a multidentate
143 phosphine oxide derivative for the uranyl (VI) ISE by the oxidation of
144 bis(diphenylphosphino)methane (CAS No. 2071-20-7). The solubility of
145 bis(diphenylphosphino)methane as a raw material was high, so 0.01 mol of the raw material was
146 suspended in 100 mL of acetone (CAS No. 67-64-1). Hydrogen peroxide (0.30 mass fraction of

147 aqueous solution, CAS No. 7722-84-1) was diluted to 0.05 mass fraction with acetone. Then,
148 diluted hydrogen peroxide (0.05 mol) was slowly added dropwise to the acetone solution in an
149 ice bath to maintain the ice temperature with stirring by a magnetic stirrer. Here, the raw
150 material was oxidized to BDPPM, which is soluble in acetone. After the suspension in acetone
151 had dissolved entirely, the acetone solution was added dropwise to a significant amount of cold
152 water, and a white solid was precipitated. After washing and drying at 80 °C in an oven, a white
153 powder of BDPPM was obtained. Tetrakis[3,5-bis(trifluoromethyl)phenyl]borate ($TFPB^-$) was
154 purified from Na^+TFPB^- (Dojindo, Japan, CAS No. 79060-88-1) and used as a supporting
155 electrolyte for the uranyl (VI) ISE. The raw material (0.02 mol of Na^+TFPB^-) was dissolved in 250
156 mL of ethanol. Then, 150 mL of distilled water was added to a mixture of the solution with slow
157 stirring, yielding a fine precipitate. The precipitate was aged for 1 h at 35 °C. After cooling the
158 mixture at ice temperature, the filtered precipitate was washed using a cold mixture of water
159 (60 mL) and ethanol (100 mL) and dried at 35 °C in a vacuum oven until the weight decrease
160 was negligible. This recrystallization process was repeated three times.

161 PAA, sulfamic acid, perchloric acid, hydrochloric acid, acetic acid, sodium hydroxide, aqueous
162 ammonia, sodium perchlorate, sodium chloride, and copper (II) perchlorate hexahydrate were
163 purchased from Wako Pure Chemical Industries (Japan), (CAS No. 9003-01-4, 5329-14-6, 7601-
164 90-3, 7647-01-0, 64-19-7, 1310-73-2, 1336-21-6, 7601-89-0, 7647-14-5, and 10294-46-9) and

used without further purification. Copper (II) perchlorate hexahydrate was dissolved in distilled water, and the concentration of Cu (II) ion solution was measured by inductively coupled plasma atomic emission spectroscopy (ICP-AES). A uranyl (VI) ion solution was prepared from U_3O_8, which was obtained from Tohoku University. The U_3O_8 powder was dissolved in nitric acid, and, then, the uranyl (VI) nitrate solution was heated on a hotplate at 180 °C. After the evaporation, hydrochloric acid was added dropwise with heating. Uranyl (VI) nitrate was converted to uranyl (VI) chloride by this process, which was repeated five times. Finally, the stock solution of uranyl (VI) chloride, for which the uranyl (VI) ion concentration was determined by ICP-AES, was prepared. In this literature, all experiments were carried out in 25 degree Celsius at 1atm, therefore, the weight of 1 cm^3 water can be regarded as 0.997 g.

2.2 Potentiometric titration

Potentiometric titration was conducted using a “Wallingford” automated titration system equipped with two automatic burettes (765 Dosimat, Metrohm, Switzerland), a water-jacketed glass vessel (6.1418.220, Metrohm), a double junction Ag/AgCl reference electrode (6.0726.100, Metrohm), a glass electrode (6.0133.100, Metrohm), and a Cu (II) ISE (6.0502.140, Metrohm). The reference electrode was filled with 3.0 mol/dm^3 sodium chloride instead of potassium chloride to avoid clogging the electrode frit glass septum on the precipitation of potassium

183 perchlorate. The glass electrode was calibrated with a standard strong acid (0.1 mol/dm^3 $HClO_4$)
184 versus standard strong base (0.1 mol/dm^3 NaOH) titration and a standard weak acid (0.1
185 mol/dm^3 CH_3COOH) versus standard weak base (0.1 mol/dm^3 NH_3) titration, where the ionic
186 strength was kept constant during the titrations at 0.1, 0.5, or 1.0 with $NaClO_4$. The sodium
187 hydroxide and ammonia solutions were standardized with 0.10 mol/dm^3 sulfamic acid. The
188 standardized and de-carbonated 0.1 mol/dm^3 NaOH solution was then used for the
189 determination of the concentrations of perchloric, acetic, and hydrochloric acids. The absolute
190 hydrogen ion concentration at each titration step of the above mentioned standard titration was
191 calculated from the mass balance equations and protonation equilibrium equations using the
192 protonation constants of hydroxide ions, acetic acid, and ammonia reported in the NIST database
193 [28]. Then, the negative logarithm of the calculated hydrogen ion concentrations, expressed as
194 pcH (=-log[H^+]) in this paper, were compared with the pH readings of the standard titrations
195 between a strong acid and strong base and weak acid and weak base at each titration step. This
196 comparison provided a linear relationship between the pH readings of the titrator and pcH over
197 a wide pH range at each ionic strength. The pH readings from the potentiometric measurements
198 were converted to the corresponding pcH values for the discussion of equilibrium using this
199 linear potentiometric relationship.
200 The Cu (II) ISE was calibrated with copper (II) perchlorate solutions of concentrations (0.003,

201 0.01, 0.03, 0.1, and 0.3) mmol/dm^3, where the sodium ion concentrations were adjusted to give
202 the same ionic strength as the titration samples. In the titration, a standardized 10 mmol/dm^3
203 NaOH solution was used as a titrant. Copper (II) perchlorate solution (2 mmol/dm^3) was used
204 as another titrant. The ionic strengths of the titrants were the same as those of the sample
205 solutions, which was achieved by adding sodium perchlorate. In this study, two types of titration,
206 i.e., a pcH-static Cu (II) ion titration and a [Cu^{2+}]-static base titration, were carried out for the
207 humic acid and PAA, where [Cu^{2+}] is the concentration of free Cu (II) ions. In the pcH-static Cu
208 (II) ion titration, log[Cu^{2+}] was increased continuously from -6 to -4 by adding the titrant
209 containing Cu (II) ions, but the pcH was maintained constant by the addition of an adequate
210 amount of NaOH solution. The volume of added NaOH solution was calculated automatically
211 using the titration system at each titration step. After each addition of the titrant, the glass
212 electrode potential was monitored at 2-min intervals. The electrode reading was recorded when
213 its drift was less than 0.1 mV/min. When the pcH was maintained within ±0.02 of its desired
214 value for 6 min, the pcH was regarded as constant, and then the glass electrode potential and Cu-
215 ISE potential were recorded as the stabilized values of the titration point. If the measured pcH
216 had not reached the desired value, the sodium hydroxide solution was added again.
217 On the other hand, in the [Cu^{2+}]-static base titration, the pcH was increased continuously from
218 4 to 7 by the addition of NaOH solution, while log[Cu^{2+}] was kept stationary by automatically

219 adding the copper (II) perchlorate solution. The volume of the added NaOH solution was set to
220 make the logarithm of the degree of dissociation of humic acid (=logα) change nearly
221 continuously. After each addition of the NaOH solution, the Cu (II) ISE potential was monitored
222 at 3-min intervals. [Cu^{2+}] was recorded when the drift was less than 0.15 mV/min. When the
223 measured log[Cu^{2+}] was maintained within ±0.03 of its desired value for 9 min, log[Cu^{2+}] was
224 regarded as stationary, and then the glass electrode potential and Cu (II) ISE potential were
225 recorded as the stabilized values of the titration point. If the measured log[Cu^{2+}] had not reached
226 the desired value, the copper (II) perchlorate solution was added again.
227
228 2.3 Preparation, calibration, and titration of the uranyl (VI) ion selective electrode
229 The liquid membrane of the uranyl (VI) ISE was prepared by solvent extraction. The aqueous
230 phase was 0.1 mol/dm^3 of hydrochloric acid containing 2 mmol/dm^3 of uranyl chloride and 6
231 mmol/dm^3 of Na^+-$TFPB^-$ as the supporting electrolyte. On the other hand, the organic phase was
232 the same volume of nitrobenzene containing 60 mmol/dm^3 of BDPPM as the ionophore. Both
233 phases were mixed in a vial by shaking for 30 min. After phase separation by centrifugation, the
234 organic phase was used to prepare the nitrobenzene solution of the UO_2 (VI)-BDPPM complex.
235 Then, the uranyl (VI) ISE was prepared in the cell configuration shown below.

236 $$\left|\begin{matrix}\mathrm{Ag/AgCl}\\ \mathrm{0.1M\ LiCl}\\ \mathrm{(SSE1)}\end{matrix}\right|\left|\begin{matrix}1\times10^{-3}\mathrm{M\ UO_2}^{2+}\\ \mathrm{(HCl\ solution)}\\ \mathrm{inner\ solution}\end{matrix}\right|\left|\begin{matrix}1\times10^{-3}\mathrm{M\ UO_2(BDPPM)_2\cdot 2TFPB}\\ \\ \mathrm{(liquid\ membrane)}\end{matrix}\right|\left|\begin{matrix}\mathrm{Test\ solution}\\ \mathrm{(HCl\ solution)}\\ \mathrm{pcH4}\ \ I=0.01\end{matrix}\right|\left|\begin{matrix}\mathrm{Ag/AgCl}\\ \mathrm{0.1M\ LiCl}\\ \mathrm{(SSE2)}\end{matrix}\right|$$

Details of the preparation and evaluation of the ISE have been given previously [27]. In this study, the pcH of the test solution was adjusted to 4, and the ionic strength was adjusted 0.01 to avoid the precipitation of humic acid. The uranyl-ISE was calibrated with uranyl chloride solutions of concentrations (0.01, 0.03, 0.1, 0.3, and 1) mmol/dm^3 in which the pcH and ionic strength were the same as those of the test solutions. The concentration of uranyl hydroxide species was calculated from hydrolysis constants in the NIST database [28]. The electrode potential was monitored by a potentiostat and recorded when its drift was less than 0.1 mV/min. The result of the calibration of uranyl (VI) ISE is shown in **Fig. 1**. The electrode response deteriorated at a uranyl chloride concentration of 0.01 mmol/dm^3, as determined from the slope; therefore, the response limit of the uranyl (VI) ISE was assumed to be 0.03 mmol/dm^3.

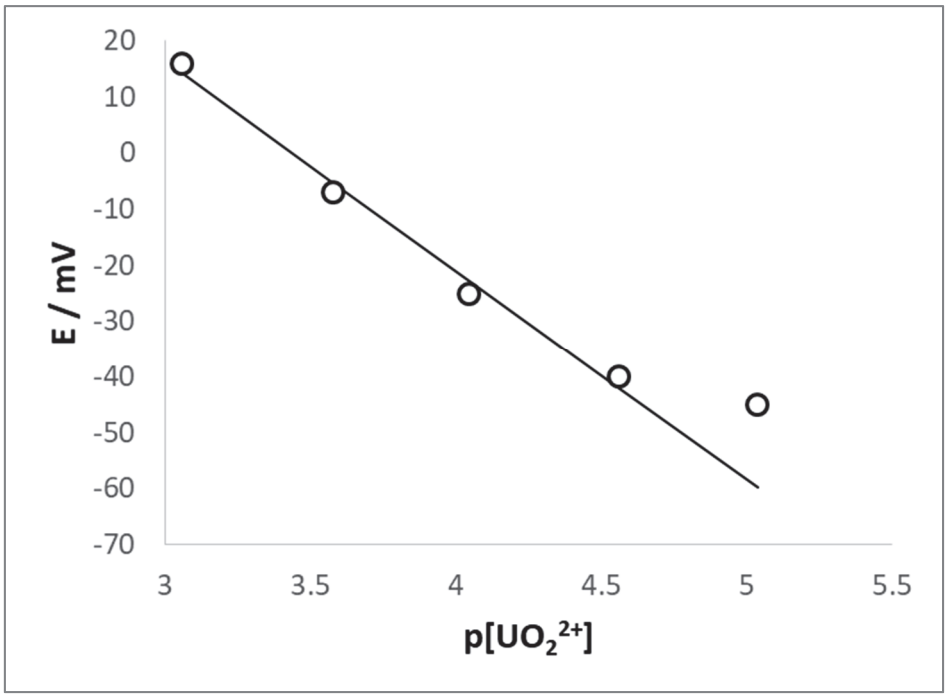

Fig. 1 Calibration of the uranyl (VI) ISE.

For the determination of the apparent complexation constant of humic acid with uranyl (VI) ions, 0.1 mmol/dm^3 of uranyl chloride solution was titrated with 500 mg/dm^3 of humic acid. The absolute hydrogen ion concentration of each titration step was calculated from the electrode potential of the glass electrode (GR-522, Hiranuma, Japan), and the uranyl (VI) ion concentration was measured by the uranyl (VI) ISE. Both values were recorded when the drift of the uranyl-ISE potential was less than 0.1 mV/min.

2.4 Calorimetric titration

Calorimetric titration was conducted with an isothermal solution calorimeter system (TAM-III, TA Instruments, USA). The titration assembly consisted of a reaction vessel (4 cm^3 volume, made from Hastelloy), which had the same volume as the reference vessel, thermoelectric devices, a calibration heater, and an 18 K gold-stirrer driven by an electric motor. The assembly was immersed in a high-precision heat sink, which maintained the temperature at (25 ± 0.000004 °C). The titrant was delivered into the reaction vessel through a titrant tube from a syringe, which was also immersed in the heat sink. The titrant volume was continuously controlled by the precision syringe pump (P/N 3810-5, TA Instruments). In the measurement of the ligand complexation enthalpy with Cu (II) ions, 3 mL of the humic acid solution and PAA were

titrated with a 2 mmol/dm^3 copper (II) perchlorate solution, in which the ionic strength was adjusted to 0.1. The titrant injection was repeated six times with 20-μL volumes in 120-min intervals. In the measurement of the complexation enthalpy with uranyl (VI) ions, 0.1 mmol/dm^3 of uranyl chloride solution was titrated with 500 mg/dm^3 of humic acid, in which ionic strength was adjusted to 0.01. The titrant injection was repeated six times with 40-μL volumes for HHA and eight times with 30-μL volumes for SHA. The interval for each injection was 120 min.

In each measurement run, the reaction heat of complexation at the *i*th titration step ($\Delta Q_{r,i}$) was obtained by subtracting the dilution heat from the heat measured by the calorimeter:

$$\Delta Q_{r,i} = \Delta Q_{ex,i} - \Delta Q_{dil,i}, \quad (1)$$

where $\Delta Q_{ex,i}$ is the heat measured by the calorimeter (J) at the *i*th addition of the titrant and $\Delta Q_{dil,i}$ is the heat consumed by the dilution of the titrant, as determined by a separate run. In this paper, the positive heat value means that the reaction system obtained a heat of $\Delta Q_{r,i}$ J from the surroundings.

3. Results

3.1 Stability constants of complexation

Because the structure of humic substances cannot be defined (they are mixtures of various heterogeneous macromolecules containing a variety of functional groups), an accurate ligand

molarity concentration cannot be defined as it would be for a simple organic acid. Therefore, we have proposed a simplified expression to describe the interaction of humic substances with cations using an apparent complexation constant determined previously [17],

$$\log K_{app}^{c} = \log K_c + a_c \log\alpha - b_c \log[\mathrm{Na^+}] - m_c \log[\mathrm{M}], \quad (2)$$

$$K_{app}^{c} = [\mathrm{ML}]/([\mathrm{M}][\mathrm{R^-}]), \quad (3)$$

where [ML] and [M] are the concentrations of bound and free cations, [R^-] is the concentration of the dissociated functional groups in the humic substances in mol/dm^3, [Na^+] is the bulk sodium ion concentration in the background electrolyte solution, which is equal to the ionic strength of the bulk solution in this study, and α is the degree of dissociation of the functional groups of humic substances (=[R^-]/[HR]+[R^-]), where the charges of metal complex and metal ion are omitted. In Eq. (2), $\log K_c$, a_c, b_c, and m_c are the characteristic constant parameters of the cations and humic substances. The value of a_c reflects the increase in the concentration of the interacting units and is expected to increase with increasing number of functional groups. The value of b_c indicates the dependence of the complexation on the ionic strength, and the value of m_c expresses the effect of site heterogeneity in cation–humic-acid interactions. The parameter $\log K_c$ is equal to the $\log K_{app}^{c}$ at $\log\alpha = \log[\mathrm{Na^+}] = \log[\mathrm{M}] = 0$. The physicochemical meaning of these parameters have been discussed previously in detail [4]. In addition, this equation has been successfully applied to the protonation of the various humic and fulvic acids in both

aqueous and non-aqueous titration system in the form of

$$\log K_{i,app}^{p} = \log K_p + m_{pi}\mathrm{pcH} - b_p \log[\mathrm{Na^+}], \quad (4)$$

$$K_{i,app}^{p} = [\mathrm{HR}]/([\mathrm{H}][\mathrm{R^-}]), \quad (5)$$

where pcH is the negative logarithm of the absolute hydrogen ion concentration (=-log[H^+]). The two groups of apparent protonation constants, $K_{1,app}^{p}$ and $K_{2,app}^{p}$, were employed for the protonation of carboxylic and phenolic groups, respectively.

To apply Eq. (2) to the complexation of humic acid with Cu (II) ions, it is necessary to know the concentration of dissociated functional groups [R^-] (or the degree of dissociation α) at each given pcH, as well as [Na^+], to calculate the apparent complexation constants. For this purpose, the base titration of the humic acid has already been carried out, and the apparent protonation constants of HHA and SHA were determined previously [11, 12]. From Eqs. (4) and (5), the degree of dissociation (=α_i) of each functional group can be expressed using the following equation as a function of pcH and [Na^+] and using three humic acid specific parameters for protonation, i.e., logK_{pi}, m_{pi}, and b_p,

$$\alpha_i = \frac{1}{1+[\mathrm{H^+}]K_{i,app}^{p}} = \frac{1}{10^{\log K_{pi}+(m_{pi}-1)\mathrm{pcH}-b_p\log[\mathrm{Na^+}]}+1}. \quad (6)$$

The parameter b_p is taken as common to the two acidic groups because this parameter is related to the charge and charge density of the macromolecule and independent of the type of functional groups. Therefore, the sum of the dissociated functional groups (R^-) is given by

$$(\mathrm{R}^{-}) = C_{\mathrm{R},1}^{\mathrm{W}}\alpha_1 + C_{\mathrm{R},2}^{\mathrm{W}}\alpha_2$$

$$= \frac{C_{\mathrm{R},1}^{\mathrm{W}}}{10^{\log K_{p1}+(m_{p1}-1)\mathrm{pcH}-b_p\log[\mathrm{Na}^{+}]}+1} + \frac{C_{\mathrm{R},2}^{\mathrm{W}}}{10^{\log K_{p2}+(m_{p2}-1)\mathrm{pcH}-b_p\log[\mathrm{Na}^{+}]}+1}, \quad (7)$$

where the first and second terms, represented by subscripts i = 1 and 2, describe the contribution from the carboxylic and phenolic groups, respectively, and $C_{\mathrm{R},1}^{\mathrm{W}}$, and $C_{\mathrm{R},2}^{\mathrm{W}}$ mean total carboxylic and phenolic group concentrations in mequiv./gram. Based on the discussion of the phenolic group capacity made previously [29], the protonation constant of phenol, i.e., log$K$ = 9.82 for I = 1.0 [28], was used as the fixed parameter of the mean protonation constant of the phenolic group (= logK_{p2}/(1-m_{p2})) in Eq. (7) for the determination of the apparent protonation constants. The determined parameters of apparent protonation constants of SHA and HHA are shown in **Table1** [11, 12].

Table 1 Obtained parameters for the protonation of humic acids and polyacrylic acid [11, 12].

	$C_{\mathrm{R},1}{}^{\mathrm{W}}$ [mequiv./g]	$\frac{\log K_{p1}}{1-m_{p1}}$	m_{p1}	b_p	$C_{\mathrm{R},2}{}^{\mathrm{W}}$ [mequiv./g]	m_{p2}	σ
SHA	4.71(7)	4.1(1)	0.60(1)	0.12(1)	1.5(1)	0.51(6)	0.05
HHA	4.07(3)	4.3(1)	-0.01(3)	-0.01(1)	1.71(7)	0.56(4)	0.06
PAA	13.94(7)	4.92(12)	0.46(1)	0.21(1)	-	-	0.32

*C_{R1},C_{R2}: total concentration of carboxylic and phenolic hydroxyl group in mequiv./g

logK_p, m_{pi}, b_p: fitting parameters for the apparent protonation constant

The digits in the parentheses following numerical values represent the estimated standard deviations () of those values in terms of the final listed digits.

To determine the apparent complexation constant from Eq. (2), HHA and SHA were titrated

in a manner such that pcH and log[Cu^{2+}] were simultaneously measured and controlled by the titration system so that any one variable (pcH or log[Cu^{2+}]) was continuously increased while keeping the other variables and [Na^{+}] constant. This titration technique enabled us to examine the Cu (II) ion–humic acid interaction as a continuous function of the free Cu (II) ion concentration or the degree of dissociation. The titration method and details have been described previously, where this apparent complexation model was applied to the complexation of humic substances with Ca (II) ion [17]. For the results of the titration, $\log K_{app}^{c}$ values of each titration point for the copper complexation were calculated using the following equation,

$$K_{app,\mathrm{Cu}}^{c} = ([\mathrm{CuL}])/([\mathrm{Cu}^{2+}][\mathrm{R}^{-}]) = ([\mathrm{Cu}^{2+}]_{\mathrm{T}} - [\mathrm{Cu}^{2+}])/([\mathrm{Cu}^{2+}][\mathrm{R}^{-}]), \quad (8)$$

where [CuL] and [Cu^{2+}] are the concentrations of bound and free Cu (II) ions, respectively, and [Cu^{2+}]$_T$ is the total concentration of Cu (II) ions. [Cu^{2+}] was directly measured from the reading of the Cu (II) ISE. Based on the hypothesis that Cu^{2+} is bound by two functional groups (= $2R^{-}$) to form a complex, [R^{-}] is derived from the following relationship,

$$[\mathrm{R}^{-}] = \left(\frac{w_{\mathrm{g}}}{V_{\mathrm{T}}}\left(C_{\mathrm{R},1}^{W} + C_{\mathrm{R},2}^{W}\right) \times 10^{-3} - [\mathrm{CuL}]\right)\alpha_{\mathrm{T}} = \left(\frac{w_{\mathrm{g}}}{V_{\mathrm{T}}}\left(C_{\mathrm{R},1}^{W} + C_{\mathrm{R},2}^{W}\right) \times 10^{-3} - 2([\mathrm{Cu}^{2+}]_{\mathrm{T}} - [\mathrm{Cu}^{2+}])\right)\alpha_{\mathrm{T}}, \quad (9)$$

where w_{g} is the weight of the humic acid dissolved in the titration vessel (g), V_{T} is the total solution volume, and α_{T} is the total degree of proton dissociation of the functional groups in humic acid, which is defined as an independent variable of [CuL]. Therefore, α_{T} was calculated

using the following function of pcH and ionic strength derived from Eq. (6) with $C_{\mathrm{R},1}^{\mathrm{W}}$, and $C_{\mathrm{R},2}^{\mathrm{W}}$ and the model parameters for the protonation, which are shown in **Table 1**,

$$\alpha_{\mathrm{T}} = \frac{[\mathrm{R}^-]}{[\mathrm{HR}]+[\mathrm{R}^-]} = \frac{1}{(C_{\mathrm{R},1}^{W}+C_{\mathrm{R},2}^{W})} \times \left(\frac{C_{\mathrm{R},1}^{\mathrm{W}}}{10^{\log \mathrm{K_{p1}}+(\mathrm{m_{p1}}-1)\mathrm{pcH}-\mathrm{b_p}\log[\mathrm{Na}^+]}+1} + \frac{C_{\mathrm{R},2}^{\mathrm{W}}}{10^{\log \mathrm{K_{p2}}+(\mathrm{m_{p2}}-1)\mathrm{pcH}-\mathrm{b_p}\log[\mathrm{Na}^+]}+1} \right). \quad (10)$$

By combining Eqs. (9) and (10), [R$^-$] can be calculated using following function of [Cu^{2+}], pcH, log[Na^+], w_g, V_T, and $[Cu^{2+}]_T$ with $C_{\mathrm{R},1}^{\mathrm{W}}$ and $C_{\mathrm{R},2}^{\mathrm{W}}$:

$$[\mathrm{R}^-] = \frac{1}{(C_{\mathrm{R},1}^{W}+C_{\mathrm{R},2}^{W})} \left(\frac{w_{\mathrm{g}}}{V_{\mathrm{T}}} \left(C_{\mathrm{R},1}^{W} + C_{\mathrm{R},2}^{W} \right) \times 10^{-3} - 2([\mathrm{Cu}^{2+}]_{\mathrm{T}} - [\mathrm{Cu}^{2+}]) \right) \times$$

$$\left(\frac{C_{\mathrm{R},1}^{\mathrm{W}}}{10^{\log \mathrm{K_{p1}}+(\mathrm{m_{p1}}-1)\mathrm{pcH}-\mathrm{b_p}\log[\mathrm{Na}^+]}+1} + \frac{C_{\mathrm{R},2}^{\mathrm{W}}}{10^{\log \mathrm{K_{p2}}+(\mathrm{m_{p2}}-1)\mathrm{pcH}-\mathrm{b_p}\log[\mathrm{Na}^+]}+1} \right). \quad (11)$$

Thus, by using Eqs. (8) and (11), the obtained titration data were compiled to yield $\log K_{app}^{c}$ and plotted against $\log\alpha_T$ or log[Cu^{2+}]. **Figs. 2**, **3**, and **4** show the results of the pcH-static titrations (α_T stationary) and [Cu^{2+}]-static titrations of PAA, SHA, and HHA, respectively. These logarithmic data were fitted to Eq. (2), where α is equal to α_T. **Table 2** shows the result of the least-squares fitting, and the solid lines in **Figs. 2**, **3**, and **4** are the calculated values from the model by using the determined parameters.

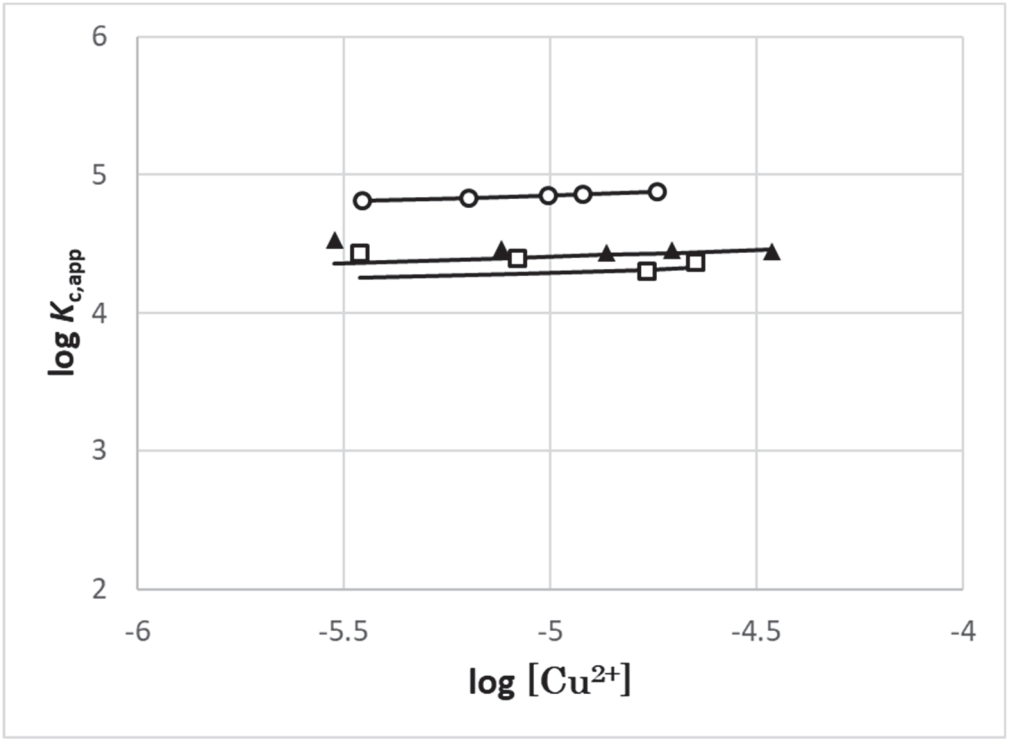

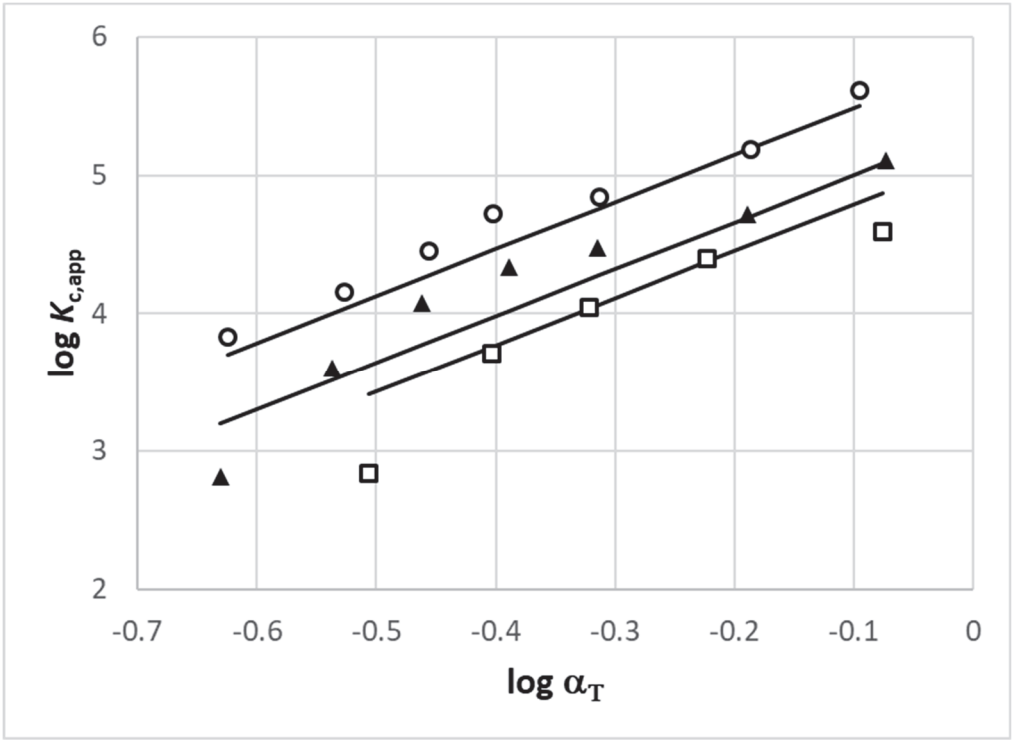

Fig. 2 Apparent complexation constants of PAA with Cu(II) as a function of (a) log[Cu^{2+}] determined by pcH-static titration and (b) logα_T by [Cu^{2+}]-static titration: ○: I = 0.1, ▲: I = 0.5, and □: I = 1.0.

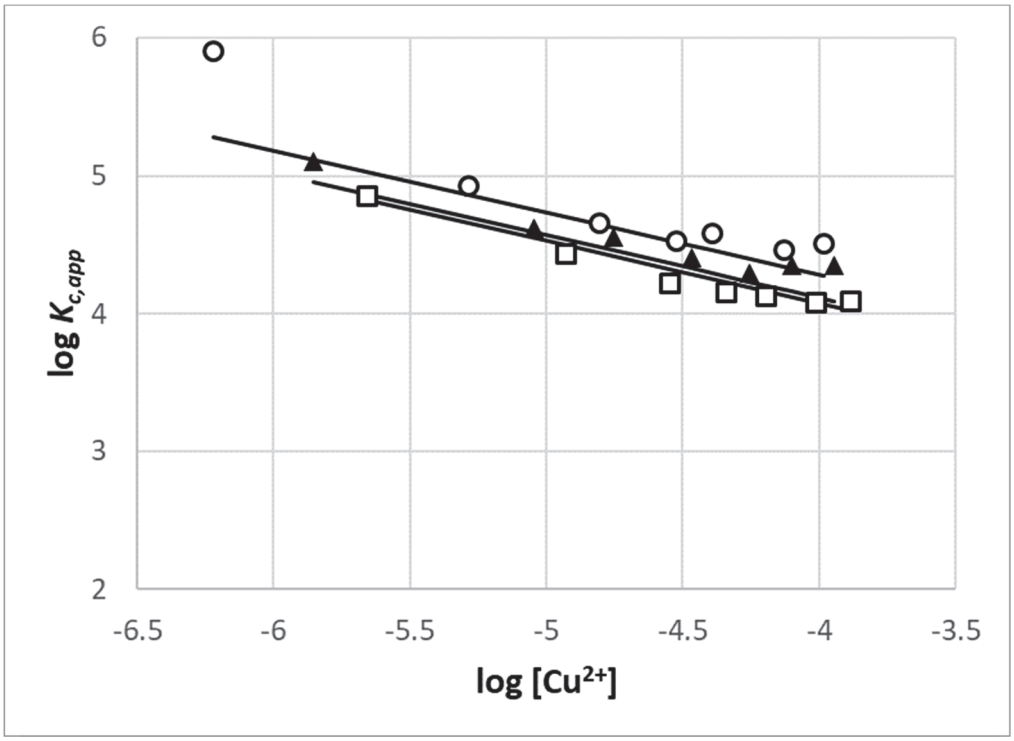

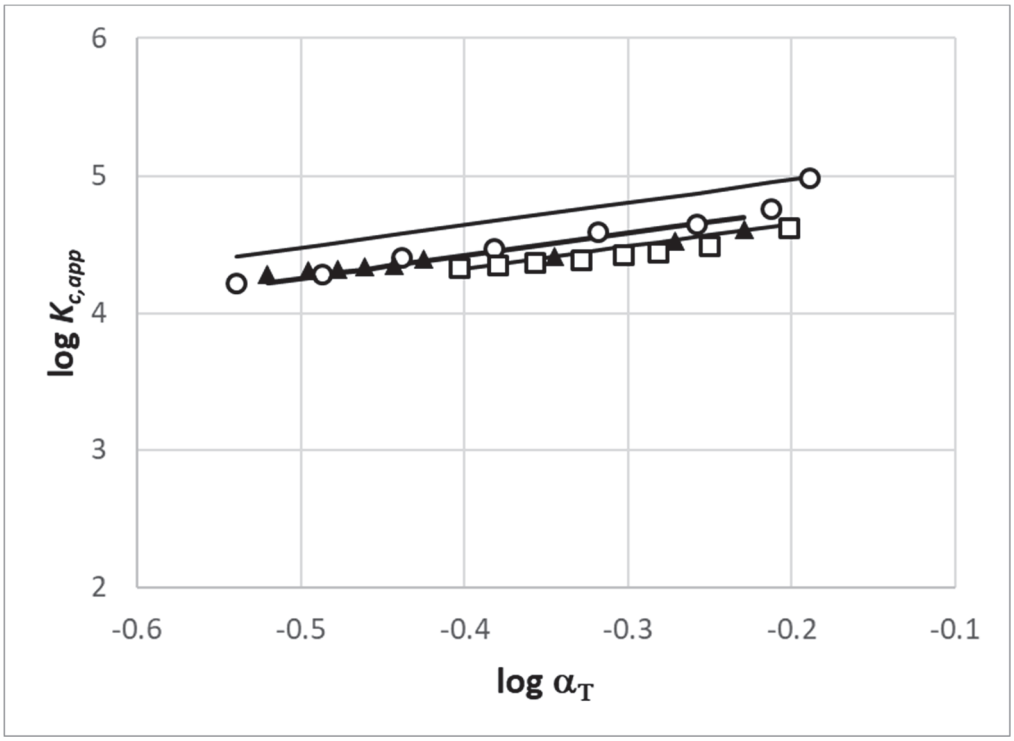

Fig. 3 Apparent complexation constants of SHA with Cu(II) as a function of (a) log[Cu^{2+}] determined by pcH-static titration and (b) logα_T by [Cu^{2+}]-static titration: ○: I = 0.1, ▲: I = 0.5, and □: I = 1.0.

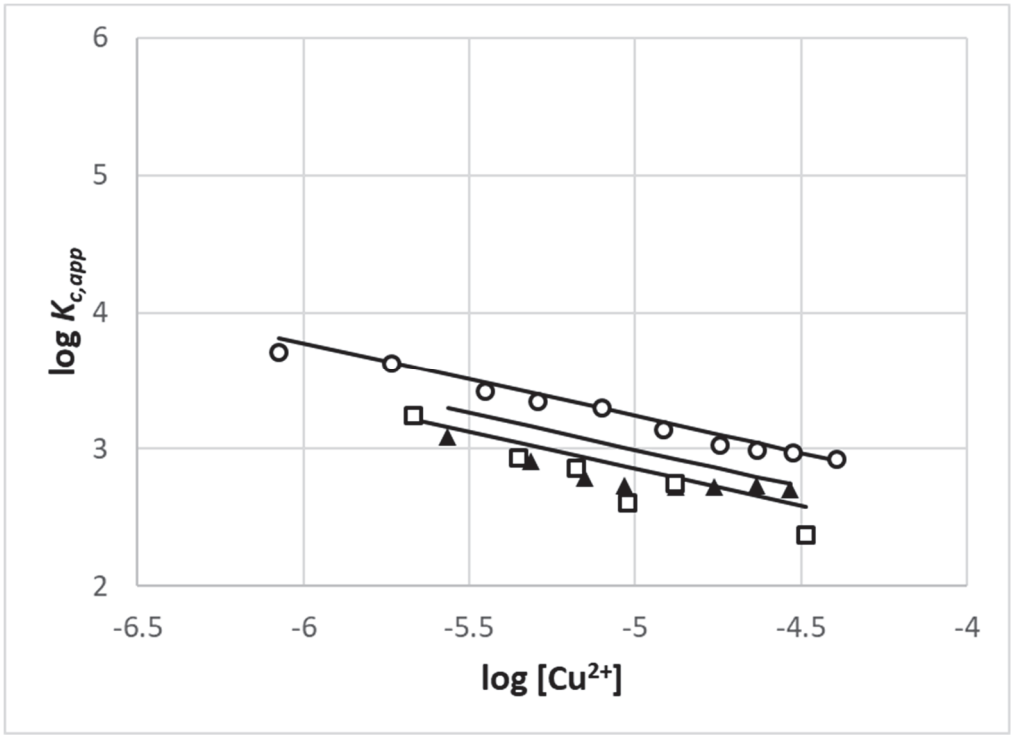

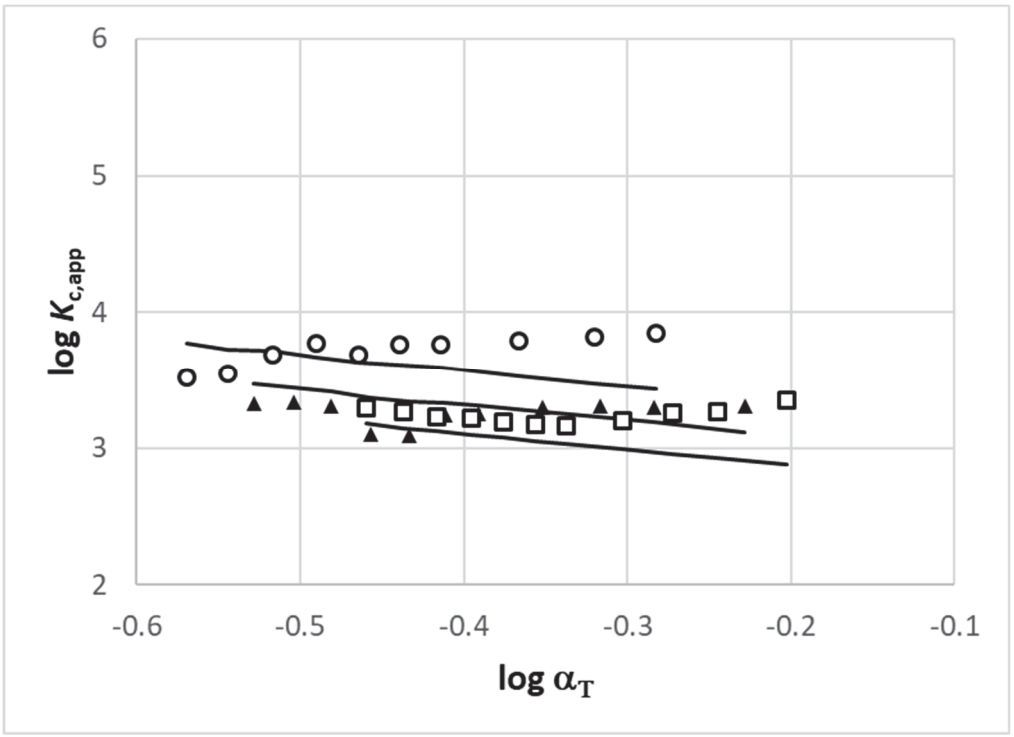

Fig. 4 Apparent complexation constants of HHA with Cu(II) as a function of (a) log[Cu^{2+}] determined by pcH-static titration and (b) logα_T by [Cu^{2+}]-static titration: ○: I = 0.1, ▲: I = 0.5, and □: I = 1.0

Table 2 Obtained parameters for the complexation of humic acid and polyacrylic acid with copper (II) ions.

	$\log K_c$	a_c	b_c	m_c	σ
SHA	2.7(2)	1.6(3)	0.31(6)	0.45(5)	0.15
HHA	-0.1(4)	-1.2(2)	0.35(6)	0.54(9)	0.23
PAA	5.6(9)	3.4(3)	0.69(9)	-0.1(2)	0.21

$\log K_c$, a_c, m_c, b_c: fitting parameters for the apparent complexation constant

The digits in the parentheses following numerical values represent the estimated standard deviations () of those values in terms of the final listed digits.

Concerning the complexation of the humic acid samples with uranyl (VI) ions, the apparent complexation constants were calculated using Eq. (12), which models the hydrolysis of uranyl (VI) ions,

$$K^{c}_{app,UO_2} = \frac{[UO_2L]}{[UO_2^{2+}][R^-]} = \frac{[UO_2^{2+}]_T - [UO_2^{2+}] - [(UO_2)_m(OH)_n^{2m-n}]}{[UO_2^{2+}][R^-]}, \quad (12)$$

where $[UO_2L]$ and $[UO_2^{2+}]$ are the concentrations of bound and free uranyl (VI) ions, respectively, $[UO_2^{2+}]_T$ is the total concentration of uranyl (VI) ion, and $[(UO_2)_m(OH)_n^{2m-n}]$ is the total concentration of uranyl (VI) hydroxide species. However, the abundance of hydroxide species is almost 7% of total uranyl (VI) ion at the experimental conditions used in this study, that is, pcH equals 4, the ionic strength is 0.01, and the total concentration of uranyl (VI) ions is 0.1 mmol/dm^3 without humic acid. Moreover, the abundance of uranyl species is reduced by complexation with humic acid; thus, Eq. (12) can be simplified following Eq. (13),

$$K^{c}_{app,UO_2} = \frac{[UO_2^{2+}]_T - [UO_2^{2+}]}{[UO_2^{2+}][R^-]}. \quad (13)$$

In this low pH range, the effect of carbonate complexation can also be negligible since it becomes

410 remarkable in pH > 6 in this experimental condition.

411 **Fig. 5** shows the results of titration in which 0.1 mmol/dm^3 of uranyl (VI) chloride solution was

412 titrated with 500 mg/dm^3 of humic acid**,** where the dotted line indicates the estimated

413 concentration of free uranyl (VI) ions, assuming no complexation between U (VI) and humic acid.

414 The decrease in the uranyl (VI) ion concentration caused by complexation with humic acid is

415 shown in this figure.

416

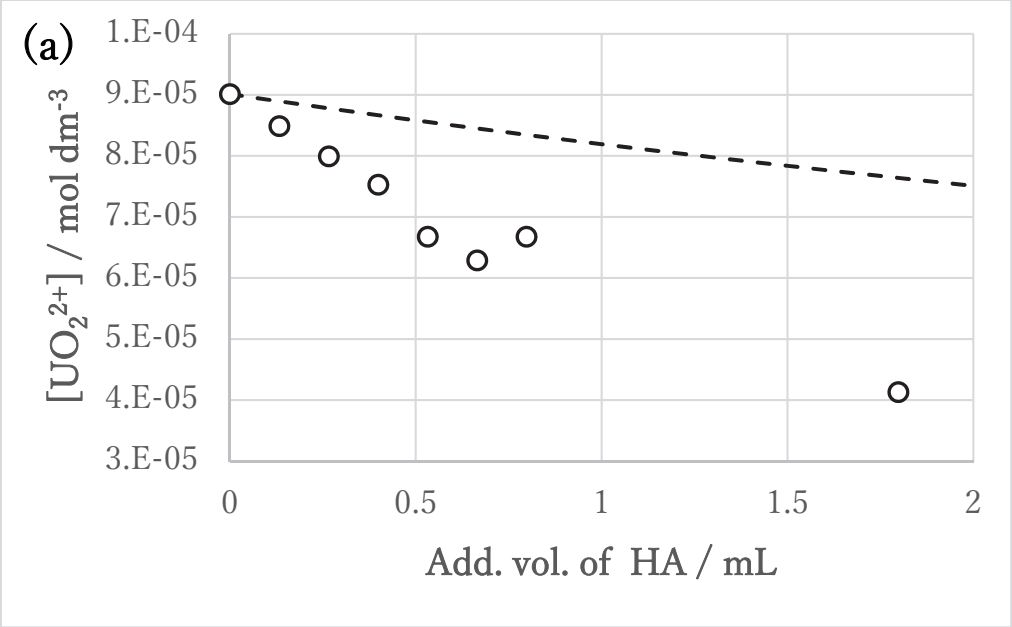

417

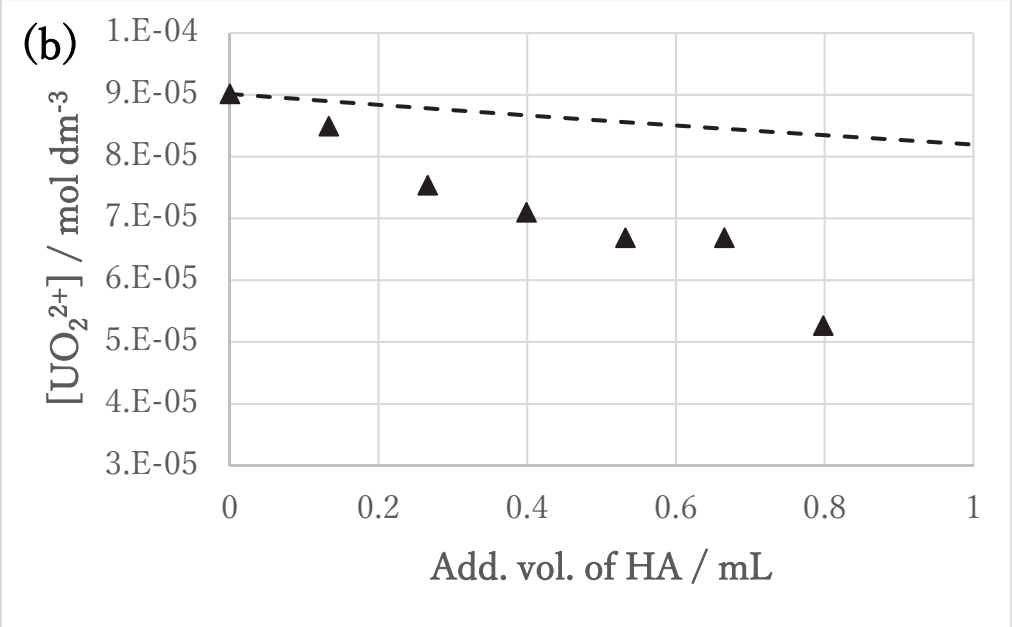

418

419 **Fig. 5** Uranyl (VI) ion concentration at each titration step of (a) SHA and (b) HHA, where the
420 dotted line indicates the estimated $[UO_2^{2+}]$ concentration change, assuming no complexation
421 between U(VI) and the humic substances, at pcH 4 and I = 0.01.
422

The apparent complexation constants of SHA and HHA with uranyl (VI) ions were calculated using Eq. (13) and are shown in **Fig. 6**. The vertical axis of **Fig. 6** is the logarithm of the apparent complexation constant, and the horizontal axis is the logarithm of the concentration of dissociated functional groups. As shown in this figure, the apparent complexation constants of both the humic acid samples increased with the increasing dissociation of functional groups. This trend is considered to reflect their heterogeneity and the polyelectrolyte effect because the same tendency was observed in the complexation with Cu (II) in **Figs. 3** and **4**.

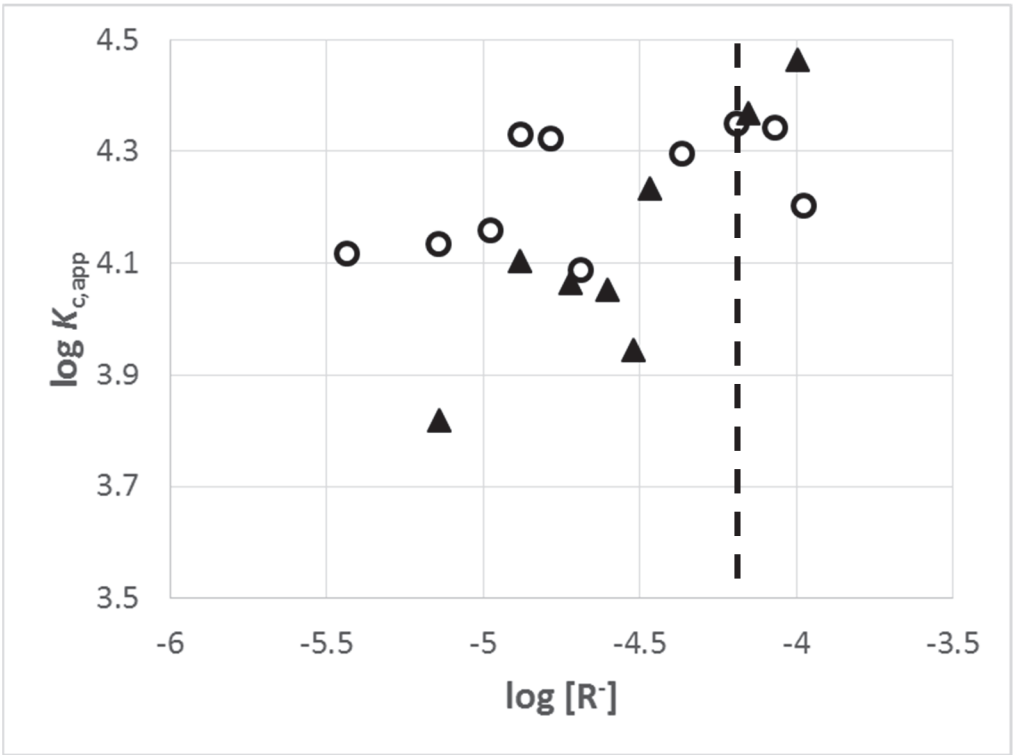

Fig. 6 Apparent complexation constants of ○SHA and ▲HHA with uranyl (VI) ions, where the dotted line is the detection limit of the ISE, at pcH 4 and I = 0.01.

435 3.2 Thermodynamic quantities of complexation

436 The apparent Gibbs free energies of complexation $\left(\Delta G_{i,app}^{c}\right)$ were calculated using Eq. (14)

437 and the complexation constants determined by potentiometric titration,

438 $$\Delta G_{i,app}^{c} = -RT \ \ln K_{i,app}^{c}. \quad (14)$$

439 The measured heat in this study contains the heat of complexation, the heat of protonation of

440 humic acid or polyacrylic acid, and the heat of neutralization of hydroxide ions. Therefore, the

441 complexation enthalpy was determined by subtracting the heat of protonation and the heat of

442 neutralization from the measured heat, as shown in Eq. (15),

443 $$\Delta H_c = \frac{\Delta Q_{r,i} - \Delta H_p \Delta \nu_{\mathrm{RH}} - \Delta H_{\mathrm{H_2O}} \Delta \nu_{\mathrm{H_2O}}}{\Delta \nu_{\mathrm{ML}}}, \quad (15)$$

444 where ΔH_{p} is the protonation enthalpy of humic acid or polyacrylic acid, which was determined

445 in a previous study [11,12]. The employed values are shown in **Table 3**.

446

447 **Table 3** Employed protonation enthalpies of SHA, HHA, and PHA at I = 0.1.

	pH	ΔH_p [kJ/mol]
SHA	4	-11.4
	5	-10.7
	6	-18.9
HHA	4 5 6	-2.4
PAA	4	4.0
	6	3.2

448

449 ΔH_{p}: protonation enthalpy

450 Uncertainties of listed values are 0.1 kJ mol^{-1}or smaller, which was checked in our

451 previous study [30].

Additionally, $\Delta\nu_{\mathrm{RH}}$ and$\Delta\nu_{\mathrm{ML}}$ are the changes in the amount of substance (moles) of protonated functional groups and that of the complexed metal cation, respectively. These values were calculated from the apparent equilibrium constants at each calorimetric titration step. In this study, the pcH of each titrant and sample solution were adjusted to the same value; thus, the total change in the pcH of the sample solution was less than 0.1. For this reason, the neutralization heat of each titration step can be neglected. The complexation entropy (ΔS) was determined by applying ΔG and ΔH to the principal equation of thermodynamics,

$$\Delta G = \Delta H - T\Delta S \quad (16).$$

In this experimental procedure, the uncertainties of determined thermodynamic quantities, which were checked in our previous study [30], are ± 0.1 kJ mol^{-1}or smaller.

From the calorimetric measurements of HAs with Cu (II) ions, the equilibrium calculations confirmed that almost all the titrated copper ions were bound by HAs; thus, the change in pCu (= -log[Cu^{2+}]) was smaller than 2.0. In addition, there was no monotonous change in the complexation enthalpies at each titration step. Therefore, the complexation enthalpies of HAs with Cu (II) ions were determined from the average value of five titration steps, except the first addition of the titrant because of the diffusion from the tip of the syringe. The thermodynamic values for the complexation of SHA, HHA, and PAA with Cu (II) ions are shown in **Fig. 7** as a bar graph at different pcH values. In addition, the median values of pCu from the calorimetric

measurements, which were used to determine ΔG and ΔS, are indicated in this graph.

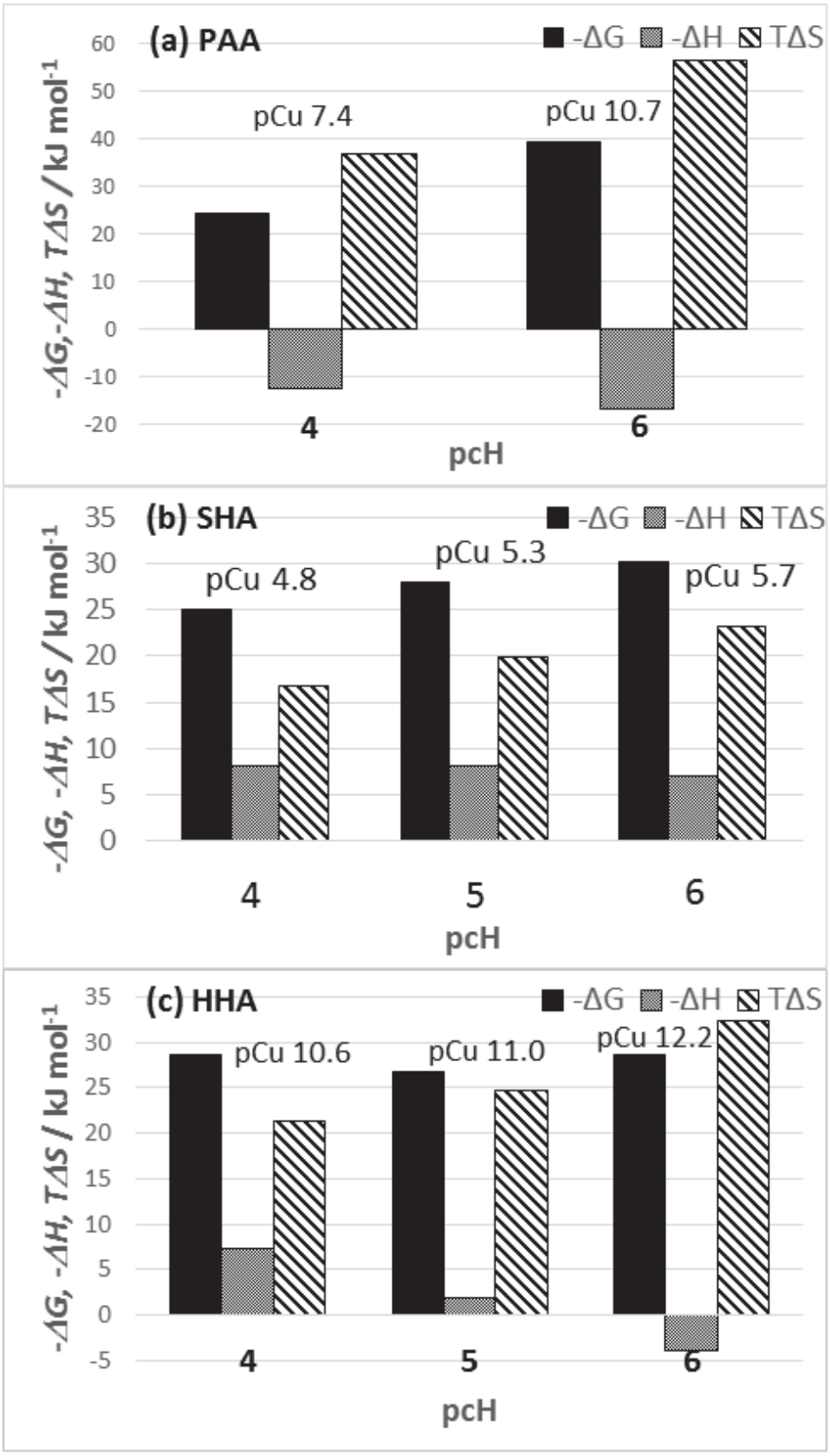

Fig. 7 Thermodynamic values for the complexation of (a) PAA, (b) SHA, and (c) HHA with Cu (II) ions, at I = 0.1, 25 degree Celsius, 1 atm.

In the calorimetric measurements of HAs with uranyl (VI) ions, the volume of added titrant was adjusted to the same scale as that of the potentiometric measurements using the uranyl (VI) ISE; thus, the change in the pcH and the uranyl (VI) ion concentration were predicted from the results of the potentiometric measurements. Then, the complexation enthalpy was calculated from the total added volume of the titrant in the calorimetric measurements. The thermodynamic quantities of complexation of SHA and HHA with uranyl (VI) ions at pH 4 are shown in **Fig. 8**. In this figure, the values of pcH and pUO_2 (=-log[UO_2^{2+}]) at the end of calorimetry, which were used to determine ΔG and ΔS, are indicated.

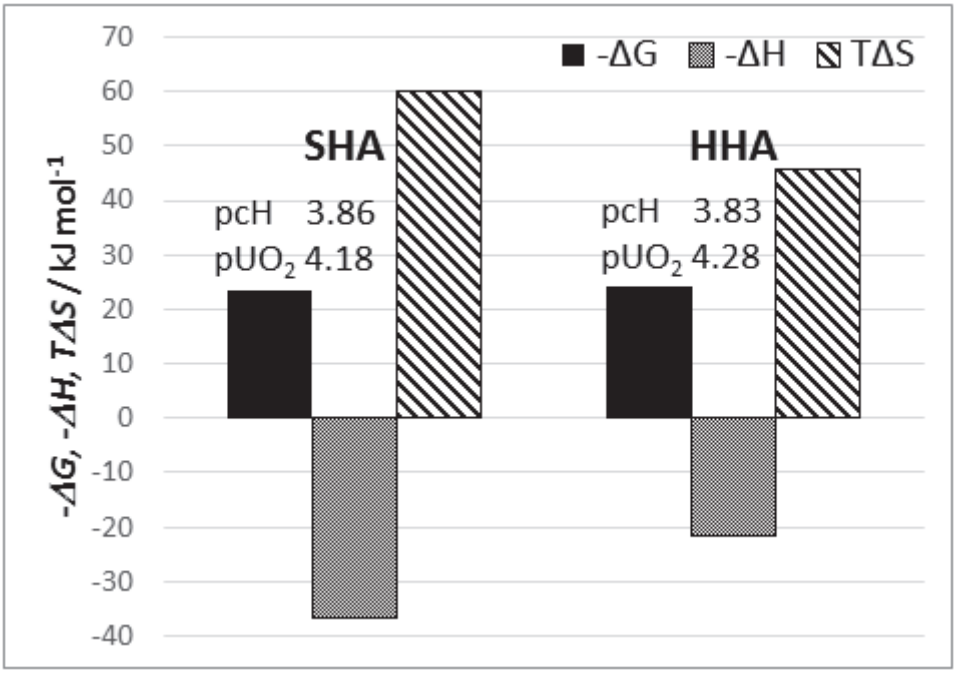

Fig. 8 Thermodynamic values for the complexation of SHA and HHA with uranyl (VI) ions at pcH 4 and I = 0.01, 25 degree Celsius, 1 atm.

4. Discussion

Fig. 2 shows the dependence of the apparent complexation constants of PAA on the free Cu (II) ion concentration and pcH of bulk solution. PAA mimics the polyelectrolyte effect of humic acid but has a homogeneous molecular structure. When the pcH of the bulk solution increases, the dissociation of the carboxyl acid groups in PAA progresses, and an accumulation of negative charge occurs at the molecular surface, which promotes protonation and complexation because of the electrostatic attraction toward cations. This characteristic of polyelectrolytes is expressed by the positive values of a_c and b_c in **Table 2** for the model equation of the apparent equilibrium constants (Eq. (2)). On the other hand, the binding energy of each functional group in PAA is almost the same because of the homogeneous structure. For this reason, the apparent complexation constants do not depend on the free Cu (II) ion concentration at a constant pcH (= constant α_T) in **Fig. 2**, as shown by the small absolute value of m_c in **Table 2**. The thermodynamic quantities of complexation of PAA with Cu (II) ion are shown in **Fig. 7**, which indicates that the complexation of PAA is driven by entropy, and the enthalpy term decreases with increasing pcH, whereas the value of the Gibbs free energy increases. The increase in ΔG can be interpreted as the polyelectrolyte effect. The negative value of $-\Delta H$ means that the sum of the dehydration energies of a free cation and dissociated functional groups is higher than the energy gained by bond formation between a cation and functional group during complexation. Therefore, the

506 complexation of PAA was driven by the entropy gain of the system arising from the increase in
507 free particles on dehydration. For a more detailed discussion of the reaction mechanism, the
508 complexation enthalpy can be determined using Eq. (17),

509 $$-\Delta H_{\mathrm{c}} = E_{\mathrm{M-L}}^{bond} - xE_{\mathrm{M-H_2O}}^{bond} - yE_{\mathrm{L-H_2O}}^{bond}, \quad (17)$$

510 where $E_{\mathrm{M-L}}^{bond}$ is the bond energy between the dissociated functional groups and the metal
511 cation, $E_{\mathrm{M-H_2O}}^{bond}$ is that of the metal cation and a water molecule, and $E_{\mathrm{L-H_2O}}^{bond}$ is that of the
512 dissociated functional group and a water molecule. At the PAA molecular surface, negative
513 charge accumulation occurs with increasing pcH. The required dehydration energy for Cu (II)
514 increases because of the possibility of the multidentate complexation of Cu (II) ion in the high
515 pcH range. However, it was hard to obtain greater enthalpy gains at high pcH because the
516 functional groups of PAA are distributed equally in the molecules, and the functional groups
517 cannot form “strong” bonds similar to those of chelating agents. This is the reason why the
518 complexation enthalpy of PAA decrease with pcH, whereas the protonation enthalpy of PAA is
519 constant [11].

520 **Figs. 3** and **4** show the dependence of the apparent complexation constants of SHA and HHA
521 on the free Cu (II) ion concentration and pcH, respectively. This indicates that the complexation
522 of SHA with Cu (II) ion is affected by both the pcH and free Cu (II) ion concentration. The reason
523 for the dependence on pcH has already been discussed as being a result of the polyelectrolyte
524 effect, similar to that of PAA. Additionally, the heterogeneity of SHA affects the dependence of

apparent complexation constants on the presence of free metal cations. Because the complexation sites in SHA molecules have a heterogeneous distribution, the formation of a complex preferentially occurs at strong bonding energy sites at low free metal ion concentrations. This is a characteristic of the complexation of humic acid, as indicated by our previous study [17]. In contrast, the complexation of HHA was estimated to be completely different from that of typical humic acids like SHA. For instance, the complexation ability of HHA with Cu (II) ions was small in comparison with SHA and PAA, as shown by the relatively small value of logK_c in **Table 2**. In addition, the small value of a_c of HHA means that the accumulation of negative charge at the molecular surface arising from the dissociation of functional groups is small in the complexation of HHA. This unique property is considered to be a reflection of the simple molecular structure: HHA has a molecular weight of about 1,000 Da, as revealed from the flow-field flow fractionation (Fl-FFF) analysis in our previous work [12]. On the other hand, the value of m_c is near 0.5 for both HHA and SHA, indicating that the distributions of the strengths of binding sites and their abundances are reasonably constant, which is a result of the heterogeneity of humic acid. This is consistent with the idea that Cu (II) ions interact mainly with two carboxylate ligands, so the values of m_c of HHA and SHA are similar.

Fig. 7 shows the thermodynamic quantities of the complexation of SHA and HHA with Cu (II) ions. In terms of SHA, -ΔG increases at high pcH, which is a reflection of the polyelectrolyte effect

543 and heterogeneity. Furthermore, -ΔH has a positive value and almost constant in this pcH range
544 (4 to 6). Therefore, the complexation of SHA with Cu (II) ions is driven by both the enthalpy and
545 entropy terms, but the contribution of the entropy term for the driving force is larger than that
546 of the enthalpy term. The entropy term also contributes to the increase in the Gibbs free energy
547 at high pcH. The constant complexation enthalpy can be interpreted by the cancelation of the
548 increase in the dehydration energy and bonding energy between the dissociated functional
549 groups and Cu (II) ions. That is, the possibility of the multidentate complexation of Cu (II) ion
550 increases with increasing pcH, thus requiring a higher dehydration energy at higher pcH, similar
551 to PAA. In contrast, the enthalpy gain also increases with increasing pcH in the complexation of
552 SHA because the Cu (II) ions can coordinate to "strong" binding sites with increasing dissociation
553 of the functional groups. As a result, both increases in the dehydration and bonding energies are
554 canceled according to Eq. (17). As a result, the complexation enthalpy is almost constant.
555 Meanwhile, there is no clear trend in the ΔG of HHA because of the negative value of a_c and the
556 positive value of m_c. However, -ΔH of HHA decreases with increasing pcH, so the complexation
557 of HHA with Cu (II) ion is driven by the entropy term. This dependence of the complexation
558 enthalpy on pcH is the same as that of PAA, which can be interpreted as a reflection of the low
559 heterogeneity of HHA, as revealed by the potentiometric measurements and our previous
560 characterization [12]. That is, the functional groups of HHA could not form "strong" bonds

561 between Cu (II) ion, even at pcH 6. Thus, the change in dehydration energy directly reflects the
562 complexation enthalpy. Consequently, the complexation mechanism of HHA, which was
563 dissolved in deep groundwater, is entirely different from that of typical humic acids.

564 **Fig. 8** shows the thermodynamic quantities of complexation of SHA and HHA with uranyl (VI)
565 ions at pcH 4 and an ionic strength of 0.01. The complexation of SHA and HHA with uranyl (VI)
566 ions is wholly driven by the entropic term, which means the dehydration energy of uranyl (VI) is
567 higher than the energy gained by the formation of the bonds in the complex. In addition, the
568 enthalpy terms of SHA and HHA were different, although the ΔG values are, coincidently, similar.
569 For a more in-depth discussion of the complexation mechanism, a comparison of the obtained
570 reaction thermodynamic quantities of SHA and HHA with protons, Cu (II) ions, and uranyl (VI)
571 ions at pcH 4 is shown in **Fig. 9**, which also shows the ionic strength and free metal ion
572 concentration. This comparison shows that the protonation enthalpies of humic acids tend to be
573 larger than their complexation enthalpies. Additionally, the complexation enthalpy of humic acid
574 with Cu (II) ion is larger than the uranyl (VI) ion.
575

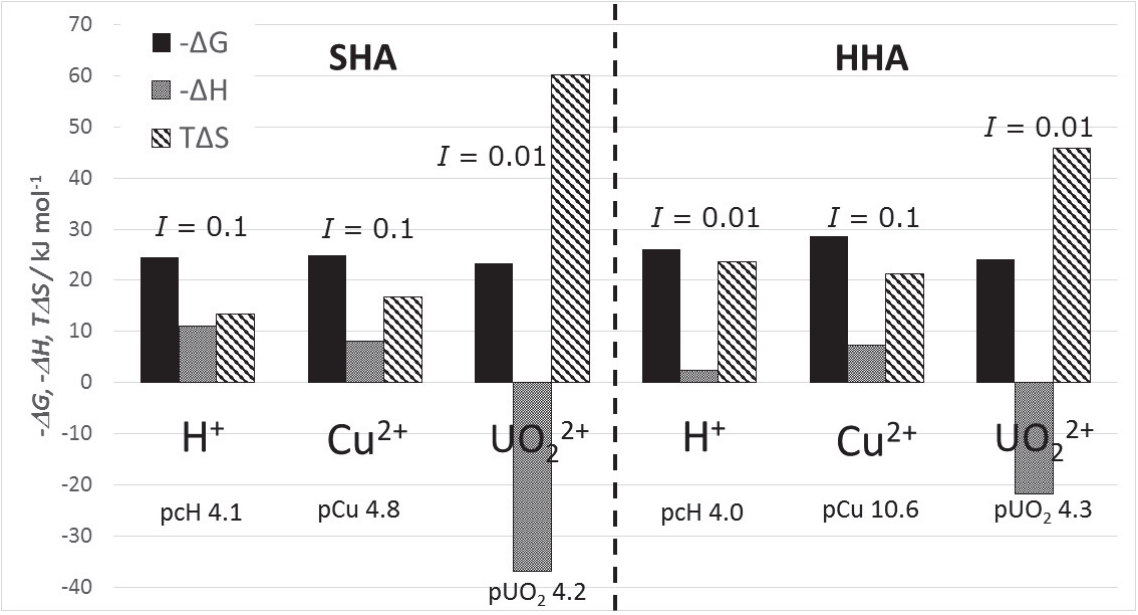

576

577 **Fig. 9** Comparison of thermodynamic quantities of SHA and HHA at pH 4, 25 degree Celsius, 1
578 atm.

579

580 This result can be attributed to the difference in the charge density, hydration number, and the
581 "softness" of cations based on HSAB theory. **Table 4** shows the ionic radius, hydration number,
582 and the "softness" of each cation [31].

583

584 **Table 4** Ionic radius, hydration number, and softness of protons, Cu (II) ions, and uranyl (VI) ions
585 [31].

	r_{I} / pm	h_{ISentr}	Softness
H^+	-	4.0	0.00
Cu^{2+}	73	9.8	0.38
UO_2^{2+}	280	15.1	-0.27

586

587

588 The proton, the simplest monovalent cation, has the smallest ionic radius and the smallest

589 hydration number; therefore, the bonding energies between the functional groups and protons
590 are higher than those of metal cations. Copper (II) is a “soft” acid, which tends to form covalent
591 bonds with functional groups having soft character, but its dehydration energy is larger than that
592 of a proton. In contrast, the uranyl (VI) ion has a large ionic radius and hydration number and is
593 a “hard” acid, tending to form ionic bonds. For this reason, the complexation enthalpy of humic
594 acids with uranyl (VI) ions is positive ($\Delta H > 0$), as shown in **Fig. 9**. In terms of HHA, the
595 protonation enthalpy value is smaller than the complexation enthalpy value for Cu (II) ions. This
596 result is regarded as a reflection of the difference between the ionic strength and concentration
597 of cations. It was revealed that the enthalpy of HHA increases with the ionic strength, which is
598 attributed to a decrease of the dehydration energy of cation at high ionic strength [12].
599 Additionally, the low concentration of Cu (II) ions arising from the high concentration of HHA
600 might be the cause of the considerable enthalpy value.

601 Consequently, the unique complexation mechanism of humic acid dissolved in deep
602 groundwater in Japan, which is not influenced by the polyelectrolyte effect and the heterogeneity,
603 was revealed by the reaction thermodynamics using the calorimetric titration technique. In
604 particular, we found that the complexation enthalpy value and trend for HHA are different from
605 those of SHA, although the value of Gibbs free energy was similar. These results show that the
606 sampling and thermodynamic investigation of dissolved humic substances in deep groundwater

607 are necessary for safety assessment when a geological disposal site is being chosen.

608

609 **5. Conclusion**

610 In this study, potentiometric titration and calorimetric titration were applied to analyze
611 humic acid dissolved in deep groundwater from Horonobe, Hokkaido for the determination of
612 thermodynamic quantities of complexation. In particular, a liquid-membrane-type uranyl (VI)
613 ion selective electrode was prepared by solvent extraction and used to determine the apparent
614 complexation constants of humic acids with uranyl (VI) ions. Consequently, the accurate
615 determination of the thermodynamic quantities of complexation of humic acids with metal
616 cations was achieved by the direct measurement of the reaction heat. By comparison of the
617 complexation enthalpies of Horonobe humic acid with that of typical humic acid and
618 homogeneous polyacrylic acid, the unique complexation mechanism, which was not affected by
619 the polyelectrolyte and heterogeneity, was revealed. This is attributed to the origin and the
620 hysteresis of Horonobe humic acid, which has experienced long-term thermal and biochemical
621 degradation. This might affect the migration of metal cations in the deep underground
622 environment. Therefore, the proposed titration methodology is suitable for the discussion of
623 reaction thermodynamics of in situ humic substances when disposal sites for radioactive waste
624 are chosen.

625

Acknowledgments

Part of this work was performed under the Research Program for the CORE Laboratory, "Dynamic Alliance for Open Innovation Bridging Human, Environment, and Materials" in "Network Joint Research Center for Materials and Devices." This work was also carried out as a cooperative study with the Japan Atomic Energy Agency (JAEA).

References

[1] F.J. Stevenson, Humus Chemistry: Genesis, Composition, and Reactions, second ed., Wiley, New York, 1994.

[2] E. Tipping, Cation Binding by Humic Substances, Cambridge University Press, Cambridge, 2002.

[3] J. Buffle, Complexation Reactions in Aquatic Systems: An Analytical Approach, Ellis Harwood, New York, 1990.

[4] O. Tochiyama, Y. Niibori, K. Tanaka, T. Kubota, H. Yoshino, A. Kirishima, B. Setiawan, Modeling of the complex formation of metal ions with humic acids, Radiochim. Acta 92 (2004) 559.

[5] C.J. Milene, D.G. Kinniburgh, W.H.V. Riemsdijk, E. Tipping, Generic NICA-Donnan model parameters for metal–ion binding by humic substances, Environ. Sci. Technol. 37 (2003) 958.

[6] B.M. Bartschat, S.E. Cabaniss, F.M.M. Morel, Oligoelectrolyte model for cation binding by humic substances, Environ. Sci. Technol. 26 (1992) 284.

[7] J. Ephraim, J.A. Marinsky, A unified physicochemical description of the protonation and metal ion complexation equilibria of natural organic acids (humic and fulvic acids). 3. Influence of polyelectrolyte properties and functional heterogeneity on the copper ion binding equilibria in an Armadale Horizons Bh fulvic acid sample, Environ. Sci. Technol. 20 (1986) 367.

[8] E. Tipping, Humic ion-binding model VI: An improved description of the interactions of

650 protons and metal ions with humic substances, Aquat. Geochem. 4 (1998) 3.

651 [9] D.G. Kinniburgh, C.J. Milne, M.F. Benedetti, J.P. Pinheiro, J. Filius, L.K. Koopal, W.H. van
652 Riemsdijk, Metal ion binding by humic acid: Application of the NICA-Donnan model, Environ.
653 Sci. Technol. 30 (1996) 1687.

654 [10] D.G. Kinniburgh, W.H. van Riemsdijk, L.K. Koopal, M. Borkovec, M.F. Benedetti, M.J. Avena,
655 Ion binding to natural organic matter: competition, heterogeneity, stoichiometry and
656 thermodynamic consistency, Colloids Surf., A 151 (1999) 147.

657 [11] S. Kimuro, A. Kirishima, N. Sato, Determination of the protonation enthalpy of humic acid
658 by calorimetric titration technique, J. Chem. Thermodyn. 82 (2015) 1.

659 [12] S. Kimuro, A. Kirishima, S. Nagao, T. Saito, Y. Amano, K. Miyakawa, D. Akiyama, N. Sato,
660 Characterization and thermodynamic study of humic acid in deep groundwater at Horonobe,
661 Hokkaido, Japan, J. Nucl. Sci. Technol. 55 (2018) 503.

662 [13] L. Rao, G.R. Choppin, Thermodynamic study of the complexation of neptunium (V) with
663 humic acids, Radiochem. Acta 69 (1995) 87.

664 [14] M.L. Antonelli, N. Calace, C. Fortini, B.M. Petronio, B.M. Pietroniro, P. Pusceddu, Calorimetric
665 investigation of complex formation of some humic compounds, J. Therm. Anal. Calorim. 70
666 (2002) 291.

667 [15] G.S.P. Alexandre, S.B. Miranda, L.F. Zara, Adsorption and thermochemical data of divalent

668 cations onto silica gel surface modified with humic acid at solid/liquid interface, J. Hazard.
669 Mater. 120 (2005) 243.
670 [16] H.H. Du, Y.P. Lin, W.L. Chen, P. Cai, X.M. Rong, Z.H. Shi, Q.Y. Huang, Copper adsorption on
671 composites of goethite, cells of Pseudomonas putida and humic acid, Eur. J. Soil Sci. 68
672 (2017) 514.
673 [17] A. Kirishima, T. Ohnishi, N. Sato, O. Tochiyama, Simplified modeling of the complexation of
674 humic substance for equilibrium calculations, J. Nucl. Sci. Technol. 47/11, (2010) 1044.
675 [18] K.R. Czerwinski, G. Buckau, F. Scherbaum, J.I. Kim, Complexation of the uranyl ion with
676 aquatic humic acid, Radiochim. Acta 65 (1994) 111.
677 [19] J.I. Kim, K.R. Czerwinski, Complexation of metal ions with humic acid: Metal ion charge
678 neutralization model, Radiochim. Acta 73 (1996) 5.
679 [20] P.M. Shanbhag, G.R. Choppin, Binding of uranyl by humic acid, J. Inorg. Nucl. Chem. 43 (1981)
680 3369.
681 [21] D. Heitkamp, K. Wagener, Kinetics of adsorption of uranium from seawater by humic acids,
682 Sep. Sci. Technol. 25 (1990) 535.
683 [22] P. Lubal, D. Fetsch, D. Široký, M. Lubalová, J. Šenkýr, J. Havel, Potentiometric and
684 spectroscopic study of uranyl complexation with humic acids, Talanta 51 (2000) 977.
685 [23] C.M. Lamy, P. Adrian, J. Berthelin, J. Rouiller, Comparison of binding abilities of fulvic and

686 humic acids extracted from recent marine sediments with UO_2^{2+}, Org. Geochem. 9 (1986)
687 285.
688 [24] S. Sachs, V. Brendler, G. Geipel, Uranium (VI) complexation by humic acid under neutral pH
689 conditions studied by laser-induced fluorescence spectroscopy, Radiochim. Acta 95 (2007)
690 103.
691 [25] T. Saito, S. Nagasaki, S. Tanaka, L.K. Koopal, Application of the NICA-Donnan model for
692 proton, copper, and uranyl binding to humic acid, Radiochim. Acta 92 (2004) 567.
693 [26] E. Tipping, S. Lofts, J.E. Sonke, Humic ion-binding model VII: A revised parameterization of
694 cation-binding by humic substances, Environ. Chem. 8 (2011) 225.
695 [27] Y. Kitatsuji, H. Aoyagi, Z. Yoshida, S. Kihara, Plutonium (III)-ion selective electrode of liquid
696 membrane type using multidentate phosphine oxide ionophore, Anal. Chim. Acta 387
697 (1999) 181.
698 [28] A.E. Martell, R.M. Smith, R.J. Motekaitis, NIST Critically Selected Stability Constants of Metal
699 Complexes, vol. 7, Texas A&M University, Texas, 2003.
700 [29] A. Kirishima, T. Ohnishi, N. Sato, Determination of the phenolic-group capacities of humic
701 substances by non-aqueous titration technique, Talanta 79 (2009) 446.
702 [30] A. Kirishima, Y. Onishi, N. Sato, O. Tochiyama, Thermodynamic study on the U(VI)
703 complexation with dicarboxylates by calorimetry, Radiochim. Acta 96 (2008) 581.

[31] Y. Marcus, Ions in Solution and their Solvation, John Wiley & Sons, 2015.

Supplementary material

Sample table

Chemical Name	Source	Initial Mole Fraction Purity	Purification Method
BDPPM[a]	synthesis	–	recrystallization
bis(diphenylphosphino)methane	Aldrich	0.97	–
TFPB[b]	synthesis	–	recrystallization
Na^+TFPB^-	Dojindo	0.99	–

[a] bis(diphenylphosphoryl)methane

[b] tetrakis[3,5–bis(trifluoromethyl)phenyl]borate

710

711 **Table. S. 1** Elemental compositions of the HHA and SHA

	Elemental composition						
Humic acid	C	H	N	O	ash	O/C	H/C
HHA	61.82	6.46	3.11	27.64	0.97	0.34	1.25
SHA	53.72	4.08	3.79	37.02	1.39	0.52	0.91

712

713

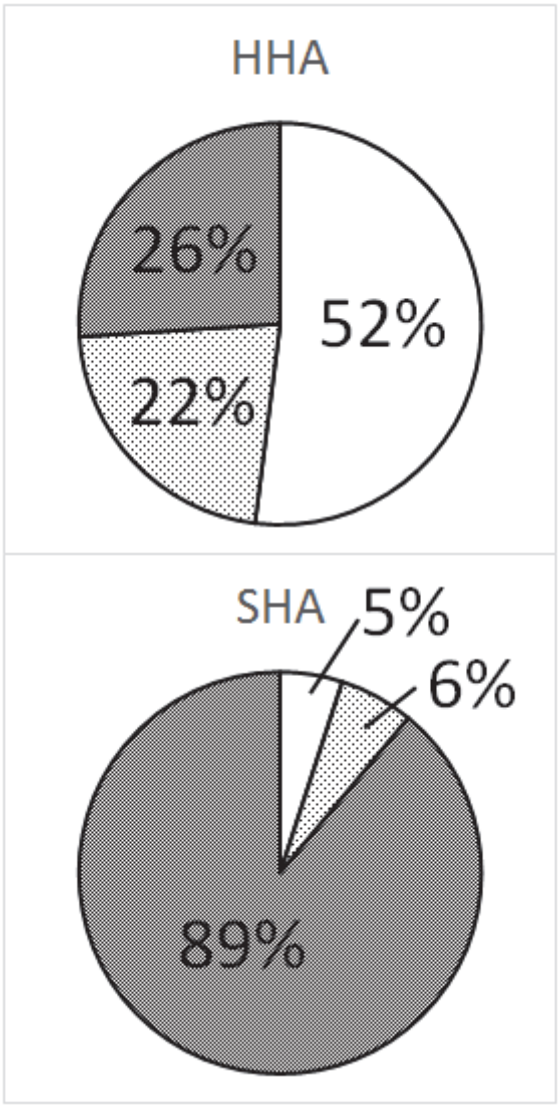

Fig. S. 1 Occupancy ratio of molecular size of HHA and SHA calculated by TOC in [12]. Note: White area: smaller than 3000 Da. Dot area: between 3000 and 5000 Da. Gray area: larger than 5000 Da.

720 Data tables for alll fiigures

721 Data for Fig.1

$p[UO_2^{2+}]$	E / mV	E_{calc}
3.059	16	14.0722
3.576	−7	−5.2515
4.044	−25	−22.7324
4.562	−40	−42.0883
5.038	−45	−59.8679

E: electrode potential

722 E_{calc}: calcrated potential by the least square fitting.

723

724 Data for Fig. 2

(a) PAA−Cu pcHstat				(b) PAA−Cu pCustat			
I	log Cu	$\log K_{c,app}$ exp	$\log K_{c,app}$ calc	I	log α	$\log K_{c,app}$ exp	$\log K_{c,app}$ calc
0.1	−5.455	4.469	4.813	0.1	−0.624	3.830	3.705
	−5.196	4.562	4.836		−0.527	4.154	4.037
	−5.003	4.600	4.854		−0.456	4.455	4.277
	−4.921	4.709	4.861		−0.402	4.724	4.461
	−4.741	4.779	4.878		−0.314	4.847	4.760
0.5	−5.521	4.526	4.362		−0.186	5.190	5.192
	−5.116	4.466	4.399		−0.095	5.609	5.502
	−4.864	4.436	4.422	0.5	−0.631	2.814	3.199
	−4.703	4.457	4.436		−0.537	3.608	3.515
	−4.463	4.446	4.458		−0.461	4.079	3.774
1.0	−5.459	4.433	4.254		−0.389	4.333	4.019
	−5.077	4.396	4.289		−0.315	4.477	4.272
	−4.766	4.299	4.317		−0.189	4.720	4.698
	−4.647	4.364	4.328		−0.073	5.105	5.090
					−0.506	2.837	3.413
					−0.403	3.707	3.761
				1.0	−0.322	4.047	4.037
					−0.223	4.398	4.375
					−0.076	4.590	4.872

I : ionic strength

α : dissociation ratio of humic acid

$K_{c,app}$: apparent complexation constant

725

726

727 Data for Fig. 3

(a) SHA–Cu pcHstat

I	log Cu	log$K_{c,app}$ exp	log$K_{c,app}$ calc
0.1	−6.221	5.906	5.284
	−5.286	4.930	4.862
	−4.806	4.654	4.645
	−4.525	4.531	4.518
	−4.392	4.585	4.458
	−4.128	4.458	4.339
	−3.983	4.511	4.273
0.5	−5.853	5.098	4.954
	−5.046	4.615	4.590
	−4.754	4.553	4.458
	−4.466	4.405	4.328
	−4.255	4.291	4.233
	−4.101	4.354	4.163
	−3.947	4.349	4.094
1.0	−5.657	4.856	4.824
	−4.926	4.434	4.494
	−4.546	4.218	4.323
	−4.341	4.157	4.230
	−4.193	4.128	4.163
	−4.011	4.082	4.081
	−3.882	4.087	4.023

(b) SHA–Cu pCustat

I	log α	log$K_{c,app}$ exp	log$K_{c,app}$ calc
0.1	−0.539	4.213	4.413
	−0.487	4.278	4.498
	−0.438	4.399	4.578
	−0.381	4.471	4.671
	−0.318	4.587	4.775
	−0.258	4.642	4.874
	−0.212	4.758	4.949
	−0.189	4.983	4.987
0.5	−0.520	4.284	4.221
	−0.495	4.308	4.262
	−0.477	4.315	4.292
	−0.461	4.341	4.318
	−0.443	4.352	4.348
	−0.425	4.389	4.378
	−0.345	4.414	4.509
	−0.271	4.524	4.629
	−0.229	4.607	4.699
1.0	−0.403	4.326	4.318
	−0.380	4.347	4.356
	−0.357	4.363	4.394
	−0.329	4.388	4.440
	−0.302	4.426	4.483
	−0.281	4.438	4.518
	−0.250	4.490	4.569
	−0.202	4.621	4.648

I : ionic strength

α : dissociation ratio of humic acid

$K_{c,app}$: apparent complexation constant

728

729

730 Data for Fig. 4

(a) HHA–Cu pcHstat

I	log Cu	log$K_{c,app}$ exp	log$K_{c,app}$ calc
0.1	−6.076	3.712	3.818
	−5.735	3.622	3.635
	−5.450	3.417	3.483
	−5.293	3.344	3.398
	−5.099	3.298	3.294
	−4.915	3.138	3.195
	−4.744	3.023	3.104
	−4.634	2.993	3.045
	−4.523	2.974	2.985
	−4.393	2.927	2.916
0.5	−5.565	3.093	3.297
	−5.316	2.908	3.164
	−5.151	2.791	3.076
	−5.034	2.731	3.013
	−4.876	2.727	2.928
	−4.762	2.727	2.867
	−4.634	2.729	2.797
	−4.533	2.708	2.744
1.0	−5.669	3.244	3.215
	−5.351	2.937	3.045
	−5.179	2.857	2.953
	−5.023	2.611	2.869
	−4.880	2.743	2.792
	−4.486	2.374	2.581

I : ionic strength

α : dissociation ratio of humic acid

$K_{c,app}$: apparent complexation constant

(b) HHA–Cu pCustat

I	log α	log$K_{c,app}$ exp	log$K_{c,app}$ calc
0.1	−0.569	3.516	3.770
	−0.545	3.550	3.726
	−0.517	3.690	3.711
	−0.490	3.769	3.671
	−0.464	3.691	3.630
	−0.439	3.759	3.616
	−0.414	3.766	3.591
	−0.367	3.794	3.531
	−0.320	3.821	3.469
	−0.283	3.847	3.434
0.5	−0.528	3.330	3.467
	−0.504	3.331	3.442
	−0.481	3.306	3.414
	−0.457	3.099	3.365
	−0.433	3.090	3.338
	−0.412	3.245	3.334
	−0.391	3.249	3.313
	−0.352	3.300	3.269
	−0.317	3.304	3.227
	−0.284	3.294	3.188
	−0.228	3.308	3.119
1.0	−0.460	3.297	3.176
	−0.437	3.262	3.147
	−0.416	3.230	3.121
	−0.395	3.217	3.097
	−0.375	3.186	3.072
	−0.356	3.175	3.051
	−0.337	3.165	3.031
	−0.303	3.200	2.994
	−0.272	3.252	2.959
	−0.245	3.264	2.925
	−0.203	3.351	2.876

731

732

733 Data for Fig. 5

	Add. vol. HA	$[UO_2^{2+}]_{read}$	$[UO_2^{2+}]_T$
(a) SHA	0	9.013E-05	9.013E-05
	0.133	8.4881E-05	8.895E-05
	0.266	7.9938E-05	8.779E-05
	0.399	7.5283E-05	8.667E-05
	0.532	6.677E-05	8.558E-05
	0.665	6.2882E-05	8.451E-05
	0.798	6.677E-05	8.347E-05
	1.798	4.1317E-05	7.639E-05
(b) HHA	0	9.0154E-05	9.015E-05
	0.133	8.4922E-05	8.897E-05
	0.266	7.5353E-05	8.782E-05
	0.399	7.098E-05	8.669E-05
	0.532	6.6862E-05	8.56E-05
	0.665	6.6862E-05	8.453E-05
	0.798	5.2642E-05	8.349E-05

734

735

736 Data for Fig. 6

	log $[R^-]$	log $K_{c,app}$
SHA	−5.440	4.120
	−5.144	4.137
	−4.981	4.160
	−4.882	4.332
	−4.787	4.324
	−4.691	4.089
	−4.369	4.298
	−4.192	4.351
	−4.070	4.344
	−3.978	4.205
HHA	−5.140	3.819
	−4.885	4.104
	−4.720	4.065
	−4.605	4.052
	−4.522	3.944
	−4.467	4.235
	−4.153	4.368
	−3.997	4.463

737

738

739 Data for Fig. 7

	pH	$-\Delta G$ / kJmol^{-1}	$-\Delta H$ / kJmol^{-1}	$T\Delta S$ / kJmol^{-1}	pCu
(a) PAA	4	24.3	−12.5	36.8	7.4
	6	39.3	−17.0	56.3	10.7
(b) SHA	4	24.9	8.1	16.8	4.8
	5	28.0	8.1	20.0	5.3
	6	30.1	6.9	23.2	5.7
(c) HHA	4	28.6	7.3	21.3	10.6
	5	26.7	1.9	24.7	11.0
	6	28.5	−3.8	32.3	12.2

740

741

742 Data for Fig. 8

	$-\Delta G$ / kJmol^{-1}	$-\Delta H$ / kJmol^{-1}	$T\Delta S$ / kJmol^{-1}
SHA	23.3	−36.8	60.2
HHA	24.1	−21.7	45.9

743

744

745 Data for Fig. 9

	SHA–H^+	SHA–Cu^{2+}	SHA–UO_2^{2+}	HHA–H^+	HHA–Cu^{2+}	HHA–UO_2^{2+}
$-\Delta G$ / kJmol^{-1}	24.5	24.9	23.3	26.1	28.6	24.1
$-\Delta H$ / kJmol^{-1}	11.1	8.2	−36.8	2.4	7.3	−21.7
$T\Delta S$ / kJmol^{-1}	13.4	16.7	60.2	23.7	21.3	45.9

746

747 *Uncertanities of thermodynamic quantities were checked by the determination of

748 complexation enthalpy of 18-crown-6 with barium chloride in our previous study

749 [30]. Thus, the uncertanities of listed value are 0.1 kJ mol^{-1}or smaller.

750 Data for Fig. S1

	Fraction	Occupancy
HHA	＜3000Da	52
	3000～5000Da	22
	＞5000Da	26
SHA	＜3000Da	5
	3000～5000Da	6
	＞5000Da	89

751